Glass transition of hard spheres in high dimensions

Bernhard Schmid and Rolf Schilling
Institut für Physik, Johannes Gutenberg-Universität Mainz, Staudinger Weg 7, D-55099 Mainz, Germany
(Received 22 December 2009; revised manuscript received 14 February 2010; published 9 April 2010)

We have investigated analytically and numerically the liquid-glass transition of hard spheres for dimensions $d\to\infty$ in the framework of mode-coupling theory. The numerical results for the critical collective and self-nonergodicity parameters $f_c(k;d)$ and $f_c^{(s)}(k;d)$ exhibit non-Gaussian k dependence even up to $d=800$. $f_c^{(s)}(k;d)$ and $f_c(k;d)$ differ for $k\sim d^{1/2}$, but become identical on a scale $k\sim d$, which is proven analytically. The critical packing fraction $\varphi_c(d)\sim d^2 2^{-d}$ is above the corresponding Kauzmann packing fraction $\varphi_K(d)$ derived by a small cage expansion. Its quadratic pre-exponential factor is different from the linear one found earlier. The numerical values for the exponent parameter and therefore the critical exponents a and b depend on d, even for the largest values of d.

DOI: 10.1103/PhysRevE.81.041502 PACS number(s): 64.70.P−, 64.70.Q−, 64.70.kj

I. INTRODUCTION

In many situations, the analytical treatment of a specific physical problem simplifies drastically if the spatial dimension d becomes infinite. For instance, it is well known that the mean-field theory for systems in thermal equilibrium becomes exact for $d=\infty$. The equation of state of a fluid can be obtained from a virial expansion. For the fluid of *hard spheres*, it has been shown that for such packing fractions φ for which the second virial term (which is proportional to φ) is finite or at most algebraically increasing with d, the third and higher-order virial terms vanish exponentially fast in the limit $d\to\infty$ [1,2].

Hard sphere systems are ideal systems to study not only equilibrium properties, but also the liquid-glass transition and glassy dynamics. The mode-coupling theory (MCT) [3] is a microscopic theory of an ideal glass transition. Knowledge of the static density correlators allows to calculate the long-time relaxation of a supercooled or supercompressed fluid and to locate the glass transition point at which the ergodic behavior in the fluid phase changes discontinuously into a nonergodic one. The experimental results for colloidal fluids, which can be modeled by hard spheres, exhibit agreement with the corresponding MCT result after the transient regime over several decades in time within 10% precision [4,5].

Properties of equilibrium phase transitions, e.g., the critical exponents at a second-order phase transition, depend strongly on the spatial dimensionality. This has motivated the investigation of the glass transition for $d=2$ [6–8] and $d=3,4$ [8–10]. The most important approximation of MCT is the factorization of the memory kernel [3]. This kernel is a *time-dependent* four-point correlator of the density modes $\rho(\vec{k})$ which is approximated by a product of time-dependent two-point correlators. This factorization resembles the mean-field approximation replacing a static two-point correlator, e.g., the spin-spin correlator $\langle S_i S_j\rangle$ for an Ising model, by a product of the order parameter, e.g., the magnetization $\langle S_i\rangle$ in case of the Ising model. Based on this analogy, MCT has been interpreted as a mean-field theory with the two-point density correlator as an order parameter [11], where spatial fluctuations of the correlation between the pair densities $\rho(\vec{r},t)\rho(\vec{r}+\vec{\delta},t+\tau)$ and $\rho(\vec{r}',t')\rho(\vec{r}'+\vec{\delta},t'+\tau)$ are neglected. In a next step, these spatial fluctuations are taken into account. Finally, it is shown that the upper critical dimension where the spatial fluctuations do not influence the critical behavior is $d_c=6$ [11] for systems without and $d_c=8$ [12,13] with conserved quantities. This implies that the square-root singularity of the nonergodicity parameter and the relation between the exponent parameter $\lambda(d)$ and the "critical" exponents $a(d)$, $b(d)$ [3] are universal above d_c [14]. However, the exponent parameter $\lambda(d)$ itself being determined by the static structure factor at the glass transition singularity depends on d. The interpretation of MCT as a mean-field model challenges the investigation of MCT with full k dependence for $d\to\infty$. As already mentioned above, analytical calculations simplify for $d\to\infty$, e.g., the leading-order term of the static and direct correlation functions for hard spheres are known and become dominant (see below). Consequently we will focus on the MCT glass transition of hard spheres in high dimensions.

Let us shortly review what is already known for hard spheres and $d\to\infty$. Taking for the direct correlation function the leading order of a virial expansion (see below), using the Vineyard approximation [15] for the normalized collective nonergodicity parameters $f(k;d)$, i.e., it is $f(k;d)\approx f^{(s)}(k;d)$, and assuming the nonergodicity parameters $f^{(s)}(k;d)$ of the self-correlator to be *Gaussian* in k with width α, a self-consistency equation for α follows from MCT. As critical packing fraction for the glass transition, it has been found [16]

$$\varphi_c^{KW}(d)\cong\sqrt{2\pi e}\,d2^{-d},\quad d\to\infty. \tag{1}$$

The replica theory for the structural glass transition [17] is another microscopic theory. It allows to calculate the Kauzmann temperature T_K or the corresponding packing fraction φ_K at which the configurational entropy per particle vanishes. Applied to hard spheres in high dimensions and performing a *small cage expansion*, it is found that [18]

$$\varphi_K(d)\cong d\,\ln(d/2)2^{-d},\quad d\to\infty. \tag{2}$$

Our main motivation is to explore the MCT scenario for $d\to\infty$, i.e., we want to investigate whether the A_2 singularity

[3] of MCT in $d=3$ survives for $d\to\infty$. Furthermore, we want to check whether the critical nonergodicity parameters $f_c(k;d)$ and $f_c^{(s)}(k;d)$ of the collective and self-correlators, respectively, are Gaussian and become equal for $d\to\infty$ and whether the critical packing fraction $\varphi_c(d)$ coincides with $\varphi_c^{KW}(d)$ and if not how it relates to the Kauzmann value $\varphi_K(d)$. In a first step, we have solved numerically the MCT equations for the *collective* and *self*-nonergodicity parameters $f(k;d)$ and $f^{(s)}(k;d)$, respectively, up to $d=800$. Inspired by the numerical solution, we have investigated in a second step the corresponding equations analytically. The outline of our paper is as follows. The next section presents the MCT equations in arbitrary dimensions d and their numerical solution for the nonergodicity parameters of the collective and self-correlator. Based on these numerical results, we present in the third section an analytic investigation of the MCT equations for hard spheres for $d\to\infty$. Section IV contains a summary and conclusions.

II. MCT EQUATIONS AND NUMERICAL SOLUTION

A. MCT equations

We consider N hyperspheres with diameter σ in a d-dimensional box with volume V. The number density is $n=N/V$ and the packing fraction

$$\varphi = nV_d(\sigma/2), \tag{3}$$

with

$$V_d(R) = \frac{\pi^{d/2}}{\Gamma(d/2+1)}R^d \tag{4}$$

the volume of a d-dimensional sphere with *radius* R. $\Gamma(x)$ is the gamma function.

MCT provides an equation of motion for the intermediate scattering function $S(k,t)$ [3]. For a one-component liquid with Brownian dynamics, the MCT equation for the normalized correlator $\phi(k,t)=S(k,t)/S(k)$ is given by

$$\gamma_k\dot{\phi}(k,t) + \phi(k,t) + \int_0^t dt' m(k,t-t')\dot{\phi}(k,t') = 0, \tag{5}$$

where γ_k is a microscopic relaxation rate related to the short-time diffusion constant. The memory kernel in bipolar coordinates reads

$$m(k,t) \equiv \mathcal{F}_k[\phi(q,t)] = \Omega_{d-1}\frac{1}{(4\pi)^d}\cdot\int_0^\infty dp\int_{|k-p|}^{k+p} dqV(k,p,q)\phi(p,t)\phi(q,t), \tag{6}$$

with the vertices in *arbitrary* dimensions d [6]

$$V(k,p,q) = n\frac{pq}{k^{d+2}}S(k)S(p)S(q)[4k^2p^2 - (k^2+p^2-q^2)^2]^{(d-3)/2}[(k^2+p^2-q^2)c(p) + (k^2-p^2+q^2)c(q)]^2, \tag{7}$$

where $c(k)$ is the direct correlation function and $\Omega_d = 2\pi^{d/2}/\Gamma(d/2)$ is the surface area of a d-dimensional unit sphere.

The corresponding equation of motion for the self-correlator $\phi^{(s)}(k,t)$ follows from Eq. (5) by replacing γ_k and $m(k,t)$ by $\gamma_k^{(s)}$ and $m^{(s)}(k,t)$, respectively. $m^{(s)}(k,t)$ is given by

$$m^{(s)}(k,t) \equiv \mathcal{F}_k^{(s)}[\phi(q,t),\phi^{(s)}(q,t)] = \frac{\Omega_{d-1}}{(4\pi)^d}\int_0^\infty dp\int_{|k-p|}^{k+p} dqV^{(s)}(k,p,q)\phi(p,t)\phi^{(s)}(q,t), \tag{8}$$

with the corresponding vertices [6]

$$V^{(s)}(k,p,q) = 2n\frac{pq}{k^{d+2}}S(p)[(k^2+p^2-q^2)c(p)]^2[4k^2p^2 - (k^2+p^2-q^2)^2]^{(d-3)/2}. \tag{9}$$

Note that the vertices Eqs. (7) and (9) reduce to the well-known expressions [3] for $d=3$ for which the triple direct correlation function $c^{(3)}(k,p,q)$ has been neglected.

B. Static correlation functions

The static correlation function $S(k)\equiv S(k,t=0)$ is related to the direct correlation function by the Ornstein-Zernike equation

$$S(k;d,\varphi) = [1-n(\varphi)c(k;d,\varphi)]^{-1}. \tag{10}$$

The direct correlation function $c(k;d,\varphi)$ is known analytically for $d\to\infty$, in case that the third and higher virial terms of the virial expansion can be neglected. It has been shown [19] that the truncation for $d\to\infty$ at the second virial term is even valid above the packing fraction at which the virial series diverges. Under these conditions, it is $c(r;d,\varphi)\cong -\Theta(\sigma-r)=f(r)$ (Mayer function) from which one obtains

$$c(k;d,\varphi)\cong c(k;d) = -(2\pi)^{d/2}\sigma^d J_{d/2}(k\sigma)/(k\sigma)^{d/2}, \tag{11}$$

where $c(k;d)$ does not depend on φ. σ is the diameter of the hard spheres and $J_n(x)$ is the Bessel function of order n. Note that the d and φ dependences of the various quantities are made explicit in cases where it is useful and suppressed otherwise. There are two d-dependent k scales on which the k variation of $S(k;d,\varphi)$ is different. For

$$\bar{k} = k\sigma/\sqrt{d}, \quad \bar{\varphi} = 2^d\varphi, \tag{12}$$

it follows from Eqs. (3), (10), and (11) by using the Taylor series for $J_{d/2}(\sqrt{d}\bar{k})$ [20] in the scaling limit $k\to\infty$, $d\to\infty$, $\varphi\to 0$ such that $\bar{k}=k\sigma/\sqrt{d}$ and $\bar{\varphi}=2^d\varphi$ are fixed

$$\lim_{d\to\infty} S[(\sqrt{d}/\sigma)\bar{k};d,2^{-d}\bar{\varphi}] = [1-\bar{\varphi}\bar{c}(\bar{k})]^{-1} \equiv \bar{S}(\bar{k};\bar{\varphi}), \tag{13}$$

where

$$\bar{c}(\bar{k}) = -\exp\left(-\frac{1}{2}\bar{k}^2\right). \tag{14}$$

Figure 1 demonstrates the convergence of $S(k;d,\varphi)$ to the scaling function $\bar{S}(\bar{k};\bar{\varphi})$ on the scale $\bar{k}$ for $\bar{\varphi}=2^d\varphi$ fixed.

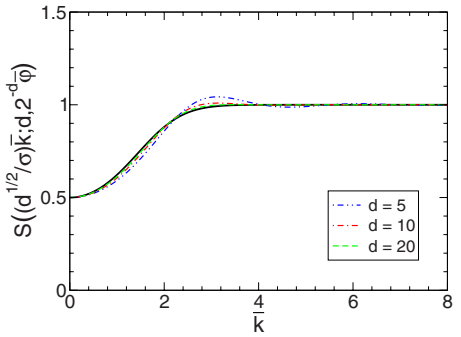

FIG. 1. (Color online) $S[(\sqrt{d}/\sigma)\bar{k};d,2^{-d}\bar{\varphi}]$ on the scale $\bar{k}$ for $\bar{\varphi}=1$ and $d=5$, 10, 20. Bold black line is $\bar{S}(\bar{k};1)$.

$\bar{S}(\bar{k};\bar{\varphi})$ does not exhibit peaks. It increases monotonically from $\bar{S}(0;\bar{\varphi})=1/[1+\bar{\varphi}]<1$ to the ideal-gas behavior $\bar{S}(\bar{k};\bar{\varphi})=1$ for $\bar{k}\to\infty$. This is the well-known effect for $k\to 0$ of the suppression of the compressibility below the corresponding value of an ideal gas which, however, is much weaker than for $d=3$.

The second k scale is linear in d,

$$\tilde{k}=k\sigma/d, \quad \tilde{\varphi}=\varphi 2^d e^{-d/2}. \tag{15}$$

Making use of the asymptotic expansion of $J_n(nx)$ [20], one obtains

$$S[(d/\sigma)\tilde{k};d,2^{-d}e^{d/2}\tilde{\varphi}]\cong[1-\tilde{\varphi}\tilde{c}_d(\tilde{k})]^{-1}\equiv\tilde{S}_d(\tilde{k};\tilde{\varphi}), \tag{16}$$

where

$$\tilde{c}_d(\tilde{k})\cong-\frac{1}{\tilde{k}^{d/2}}(1-4\tilde{k}^2)^{-1/4}\exp\left[-\frac{d}{2}(\operatorname{arctanh}\sqrt{1-4\tilde{k}^2}-\sqrt{1-4\tilde{k}^2})\right] \tag{17}$$

for $\tilde{k}<1/2$ and

$$\tilde{c}_d(\tilde{k})\cong-\frac{2}{\tilde{k}^{d/2}}(4\tilde{k}^2-1)^{-1/4}\cos\left[\frac{d}{2}\sqrt{4\tilde{k}^2-1}-\frac{d}{2}\arctan\sqrt{4\tilde{k}^2-1}-\frac{\pi}{4}\right] \tag{18}$$

for $\tilde{k}>1/2$. $\tilde{S}_d(\tilde{k};\tilde{\varphi})$ oscillates for $\tilde{k}>1/2$.

The position $k_*(d)$ of the main peak (first sharp diffraction peak) of $S(k;d,\varphi)$ is given by the first nonvanishing zero of $J_{d/2+1}(x)$, which is [20]

$$k_*(d)\cong(d/2+1)+a_0(d/2+1)^{1/3}, \quad a_0=1.855\,757\,1. \tag{19}$$

Since $k_*(d)$ and $c(k;d)$ from Eq. (11) are φ independent, the packing fraction $\varphi_*(d)$ for which $S[k_*(d);d,\varphi]$ diverges follows from Eqs. (3), (4), and (10)

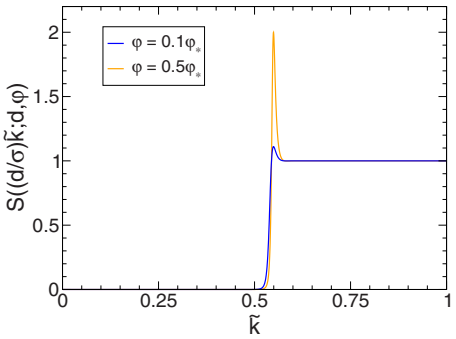

FIG. 2. (Color online) $S[(d/\sigma)\tilde{k};d,\varphi]$ vs $\tilde{k}$ for $d=200$ and $\varphi=0.1\varphi_*$, $\varphi=0.5\varphi_*$.

$$\varphi_*(d)=\frac{\pi^{d/2}(\sigma/2)^d}{\Gamma(d/2+1)c[k_*(d);d]}. \tag{20}$$

Using again the asymptotic properties of the gamma and Bessel function and especially from [20]

$$J_{d/2}[k_*(d)]=J'_{d/2+1}[k_*(d)]\cong-b_0(d/2+1)^{-2/3},$$

$$b_0\cong 1.113\,102\,8, \tag{21}$$

we obtain

$$\varphi_*(d)\cong c_0 d^{1/6}\exp[a_0(d/2)^{1/3}](\sqrt{8/e})^{-d},$$

$$c_0=b_0^{-1}\pi^{-1/2}2^{-2/3}e\cong 0.867\,956, \tag{22}$$

i.e., the leading d dependence of $\varphi_*(d)$ is the exponential factor $(\sqrt{8/e})^{-d}\cong(1.7155)^{-d}$ [21]. Note that $S(k;d,\varphi)>0$ for all k provided $\varphi<\varphi_*(d)$. For $\varphi\ll\varphi_*(d)$, the height of the first sharp diffraction peak of $S(k;d)$ is given as

$$S[k_*(d);d,\varphi]\cong 1+\frac{\varphi}{\varphi_*(d)}. \tag{23}$$

Figure 2 presents $S(k;d,\varphi)$ on the scale $\tilde{k}=k\sigma/d$ for $d=200$ and φ of order $\varphi_*(d)$.

$S[(d/\sigma)\tilde{k};d,\varphi]$ is practically zero for $\tilde{k}\lesssim 0.5$, develops its main peak at $\tilde{k}_*(d)=k_*(d)\sigma/d$, and decays very fast to one for $\tilde{k}>\tilde{k}_*(d)$. In contrast to this, Fig. 3 shows $S[(d/\sigma)\tilde{k};d,\varphi]$ again on the scale $\tilde{k}$ but for φ of order $\varphi_c(d)\cong 0.22d^2 2^{-d}$,

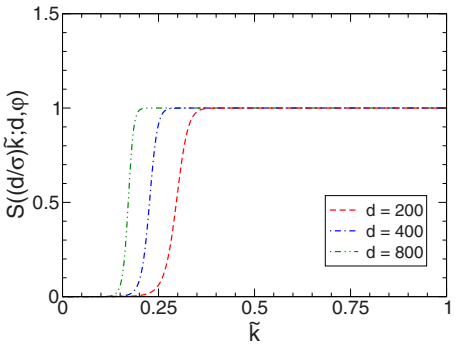

FIG. 3. (Color online) $S[(d/\sigma)\tilde{k};d,\varphi]$ vs $\tilde{k}$ for $d=200$, 400, 800 and $\varphi=\varphi_c(d)$.

which will turn out to be the critical packing fraction of the MCT glass transition. Note that $\varphi_c(d)$ is exponentially smaller than $\varphi_*(d)$.

Except for $\tilde{k}=O(1/\sqrt{d})$ which is $k\sigma=O(\sqrt{d})$, it is $S(k;d,\varphi)\cong 1$, i.e., the static structure factor on a k-scale *linear* in d is very close to that of an ideal gas for $d\to\infty$. The first sharp diffraction peak of the conventional liquids has disappeared due to the lack of intermediate range order at $\varphi=\varphi_c(d)$. These results will be used for the analytical treatment of the MCT equation. It is important to note that $[S(k;d,\varphi)-1]$ is very small for $k\sigma=O(d)$, $\varphi=O[\varphi_c(d)]$, and $d\gg 1$, but not zero. Accordingly, the direct correlation function does not vanish, in contrast to an ideal gas with finite density. Therefore, the vertices Eqs. (7) and (9) are nonzero and exhibit nontrivial k dependence.

C. Numerical solution

The nonergodicity parameter for the collective correlator is the long-time limit of the normalized intermediate scattering function

$$f(k;d,\varphi)=\lim_{t\to\infty}\phi(k,t;d,\varphi) \tag{24}$$

and similarly for the self-correlator

$$f^{(s)}(k;d,\varphi)=\lim_{t\to\infty}\phi^{(s)}(k,t;d,\varphi). \tag{25}$$

They are the order parameters for the liquid-glass transition. From Eq. (5) and the corresponding equation for $\phi^{(s)}(k,t;d,\varphi)$, one obtains the algebraic, nonlinear equations for the nonergodicity parameters

$$f(k;d,\varphi)/[1-f(k;d,\varphi)]=\mathcal{F}_k[f(q;d,\varphi);d,\varphi] \tag{26}$$

and a similar equation for $f^{(s)}(k;d,\varphi)$ by replacing $\mathcal{F}_k$ by $\mathcal{F}_k^{(s)}$. Note that we also made explicit the d and φ dependences of the functional $\mathcal{F}_k$ on the right-hand side of Eq. (26). Equation (26) and the corresponding one for $f^{(s)}(k;d,\varphi)$ have been solved numerically as follows.

Equation (26) is rewritten such that the nonergodicity parameters $f(k;d,\varphi)$ can be evaluated by iterating the equation

$$f^{(i+1)}(k;d,\varphi)=\frac{\mathcal{F}_k[f^{(i)}(q;d,\varphi);d,\varphi]}{\mathcal{F}_k[f^{(i)}(q;d,\varphi);d,\varphi]+1}, \tag{27}$$

with the initial value

$$f^{(0)}(k;d,\varphi)\equiv 1 \tag{28}$$

and similar equations for $f^{(s)}(k;d,\varphi)$. Note that in case of hard spheres, the functional $\mathcal{F}_k$ for the zero-order iterate $f^{(0)}(k;d,\varphi)$ from Eq. (28) exists only for a finite cutoff at $k_{\max}$. The integrals appearing in $\mathcal{F}_k[f^{(i)}(k;d,\varphi);d,\varphi]$ are replaced by Riemann sums with an upper cutoff $\sigma k_{\max}=\max(40d^{1/2};4d;0.2d^{3/2})$ and 500 gridpoints for $d<200$, 1000 gridpoints for $200\le d\le 600$, and 1500 gridpoints for $d>600$. The critical packing fraction $\varphi_c(d)$ is the packing fraction, where

$$f(k;d,\varphi)\begin{cases}=0, & \varphi<\varphi_c(d)\\ \neq 0, & \varphi\ge\varphi_c(d)\end{cases} \tag{29}$$

and the critical nonergodicity parameters are given by

$$f_c(k;d)\equiv f[k;d,\varphi_c(d)]. \tag{30}$$

Because the real critical packing fraction and the critical nonergodicity parameters can never be computed numerically in finite time, we evaluated $f_c(k;d)$ at a packing fraction $\hat{\varphi}_c(d)$ where $\lim_{i\to\infty}f^{(i)}[k;d,\hat{\varphi}_c(d)]=0$ but

$$\min_i\left\{\max_k\left|\frac{f^{(i+1)}[k;d,\hat{\varphi}_c(d)]-f^{(i)}[k;d,\hat{\varphi}_c(d)]}{f^{(i+1)}[k;d,\hat{\varphi}_c(d)]}\right|\right\}<\varepsilon, \tag{31}$$

with $\varepsilon=10^{-7}$ for $d\le 600$ and $\varepsilon=10^{-5}$ for $d>600$. It can be estimated that the relative difference between this packing fraction $\hat{\varphi}_c(d)$ and the real critical packing fraction $\varphi_c(d)$ is of order ε. It has been verified that the system really becomes nonergodic near this packing fraction, i.e., $f(k;d,\varphi)\neq 0$ for $\varphi>[1+\varepsilon O(1)]\hat{\varphi}_c(d)$. The critical nonergodicity parameters can then be approximated by $f_c(k;d)\cong f^{(i_0)}[k;d,\hat{\varphi}_c(d)]$, where i_0 equals the iteration step, where

$$\max_k\left|\frac{f^{(i_0+1)}[k;d,\hat{\varphi}_c(d)]-f^{(i_0)}[k;d,\hat{\varphi}_c(d)]}{f^{(i_0+1)}[k;d,\hat{\varphi}_c(d)]}\right| \tag{32}$$

reaches a minimum [24]. It has been verified that there are no visible differences in the critical nonergodicity parameters obtained by this procedure with different values of ε and that $f[k;d,\varphi_c(d)+\Delta\varphi]$ converges to $f^{(i_0)}[k;d,\hat{\varphi}_c(d)]$ with order $\sqrt{\Delta\varphi}$. Additionally, it has been verified that $f_c(k_{\max};d)<10^{-16}$ for all evaluated dimensions. By increasing $k_{\max}$ and the number of gridpoints, the relative error of the critical packing fraction due to the discretization can be estimated to be smaller than 10^{-3} for $d\le 600$.

The nonergodicity parameters always show numerical artifacts on the first few gridpoints in k space. This is a problem when trying to observe the characteristics of $f_c(k;d)$ for small wave numbers, especially for high dimensions. So we interpolated $f_c(k;d)$ onto a much finer k grid and performed one single iteration step equivalent to the one given in Eq. (27). This procedure improves the result for $f_c(k;d)$ by shifting the numerical artifacts to much smaller values of k.

From this solution, we obtain the critical packing fraction $\varphi_c(d)$, shown in Fig. 4. The d dependence of φ_c can be well fitted by

$$\varphi_c(d)\cong ad^2 2^{-d},\quad a\cong 0.22. \tag{33}$$

The critical nonergodicity parameters $f_c(k;d)$ and $f_c^{(s)}(k;d)$ are presented in Figs. 5(a) and 5(b), respectively, for different values of d. Figures 5(a) and 5(b) reveal the following properties:

(i) $f_c(k;d)$ and $f_c^{(s)}(k;d)$ differ on the scale $k\sigma=O(\sqrt{d})$, but become identical on the scale $k\sigma=O(d)$, for d large enough.

(ii) Both, $f_c(k;d)$ and $f_c^{(s)}(k;d)$, exhibit *non-Gaussian* k dependence.

(iii) There are three characteristic k scales. $f_c(k;d)$ increases from $f_c(0;d)$ to its maximum value on a scale $k\sigma\sim\sqrt{d}$, develops a plateau on a scale $k\sigma\sim d$, and it varies on a

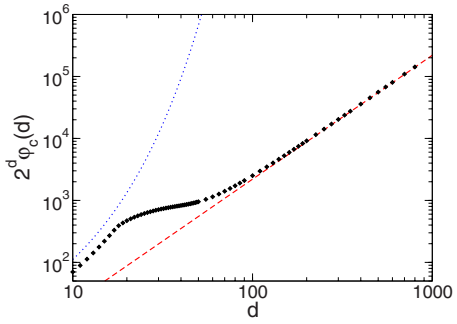

FIG. 4. (Color online) d dependence of the critical packing fraction $\varphi_c(d)$ on a log-log representation. Dashed line is $2^d\varphi_c(d) \cong ad^2$. Dotted line is $\varphi_*(d)$ from Eq. (20).

scale $k\sigma \sim d^{3/2}$, on which a steep descent to zero occurs for $k\sigma \cong \hat{k}_0 d^{3/2}$, where $\hat{k}_0 \cong 0.15$. The plateau value on scale $k\sigma \sim d$ converges to one for $d \to \infty$.

(iv) Since $f_c(k;d)$ changes from 1 to zero around $k\sigma \cong \hat{k}_0 d^{3/2}$, we will choose $\hat{k}_0$ such that $f_c(\hat{k}_0 d^{3/2}/\sigma;d) = 1/2$. $f_c(k;d)$ is of order 1 for $(k\sigma - \hat{k}_0 d^{3/2})$ of order $d^{1/2}$, i.e., for $(\tilde{k} - \hat{k}_0 d^{1/2})$ of order $d^{-1/2}$.

Using Eq. (26), $f_c(0;d)$ can be represented as a functional of $f_c(k;d)$ [6]. Making use of this relationship yields the numerical precise values for $f_c(0;d)$ shown by diamonds in Fig. 5(a). Note that for the self-correlators, it is $f_c^{(s)}(0;d) = 1$ for all d because the momentum of a tagged particle is not conserved.

A crucial quantity of MCT is the exponent parameter $\lambda(d)$ which determines the critical exponents of both power laws in time, the critical law and the von Schweidler law, and the divergence of the corresponding relaxation-time scales at the glass transition singularity [3]. Figure 6 presents the numerical result for $\lambda(d)$ with an estimated relative error of about 5×10^{-3} for $d \leq 600$ and possibly a larger error for $d = 700$ and 800.

Since the direct correlation function (11) is not correct for small d, the variation of λ with d below 100 and particularly the high sensitivity close to $d = 17$ is an artifact of the incorrect static input. This holds also for $\varphi_c(d)$ of Fig. 4. The concave curvature of $\varphi_c(d)$ and the cusplike behavior of $\lambda(d)$

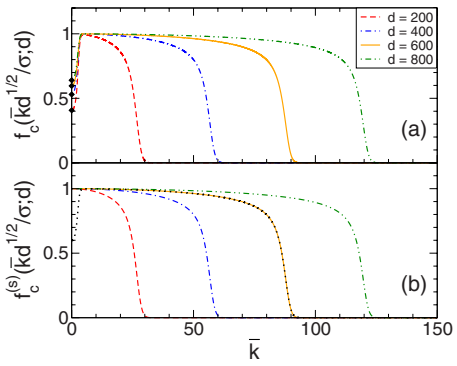

FIG. 5. (Color online) $\bar{k}$ dependence of the critical nonergodicity parameters (a) $f_c(k;d)$ and (b) $f_c^{(s)}(k;d)$ for $d = 200$, 400, 600, and 800. Diamonds in (a) mark the numerical precise values for $f_c(0;d)$ and the dotted line in (b) presents $f_c(k;600)$.

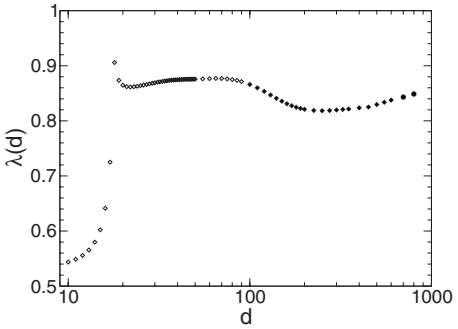

FIG. 6. d dependence of the exponent parameter λ. Full symbols mark the regime where $\varphi_c(d)$ from Fig. 4 follows the asymptotic result (33). The values for $d = 700$ and 800 depicted by full circles possibly have a larger relative error.

around $d = 17$ relates to the fact that the glass transition is still influenced by the main diffraction peak of the static structure factor for $d \lesssim 17$, while this peak is not important anymore for $d \gtrsim 17$. Figure 4 reveals the correct asymptotic d dependence to appear for $d \gtrsim 100$.

III. MCT EQUATIONS: ANALYTICAL APPROACH

In this section, we will demonstrate that the MCT functional $\mathcal{F}_k$ strongly simplifies for $d \to \infty$. The essential steps will be given, only.

In the first step, we rewrite $\mathcal{F}_k[f(q)]$ [Eq. (6) with $\phi(q,t)$ replaced by the nonergodicity parameters $f(q)$] on the scale $\tilde{k} = k\sigma/d$. Quantities on this scale will be denoted by a tilde, e.g., $\tilde{f}(\tilde{k})$. Now, we prove that $\mathcal{F}[f(q)]$ on this scale reduces to $\mathcal{F}_k^{(s)}$ for $\tilde{k}$ of order 1 and larger.

The last square bracket in Eq. (7) contains a mixed term $\sim c(\tilde{p}d/\sigma)c(\tilde{q}d/\sigma)$ which is oscillating in $\tilde{p}$ and $\tilde{q}$ faster and faster under an increase of d. Since $S(\tilde{p}d/\sigma)S(\tilde{q}d/\sigma)$, and $f(\tilde{p}d/\sigma)f(\tilde{q}d/\sigma)$ are smooth and not strongly oscillating (see Sec. II), the mixed term integrated over $\tilde{p}$ and $\tilde{q}$ will not contribute for $d \to \infty$. Taking account of this fact and using the integrand's symmetry with respect to $\tilde{p} \leftrightarrow \tilde{q}$, we get for $d \to \infty$ the MCT functional Eq. (6) but with the replacement

$$V(\tilde{k}d/\sigma, \tilde{p}d/\sigma, \tilde{q}d/\sigma) \to S(\tilde{k}d/\sigma)S(\tilde{q}d/\sigma)V^{(s)}(\tilde{k}d/\sigma, \tilde{p}d/\sigma, \tilde{q}d/\sigma) \to V^{(s)}(\tilde{k}d/\sigma, \tilde{p}d/\sigma, \tilde{q}d/\sigma). \quad (34)$$

The latter step in Eq. (34) uses $S(\tilde{k}d;d) \to 1$ for $d \to \infty$ and $\tilde{k}$ of order 1 or larger. Remember that this does not hold for $\tilde{k} = O(1/\sqrt{d})$ (see Sec. II B). Equation (34), together with the Vineyard approximation for $\phi(\tilde{p}d/\sigma, t)$ in $\mathcal{F}_k^{(s)}$ [Eq. (8)], implies that the MCT equations for the self-correlator and collective correlator on a k-scale linear in d become identical for $d \to \infty$. However, for large but finite d, there is an interval $k\sigma \in [0, O(\sqrt{d})]$ for which both MCT functionals differ from each other.

Having reduced V to $V^{(s)}$ on the k-scale linear in d further simplifications occur due to $d \to \infty$. First of all, we can replace $S(\tilde{p}d/\sigma)$ in $V^{(s)}(\tilde{k}d/\sigma, \tilde{p}d/\sigma, \tilde{q}d/\sigma)$ by 1. The product of both square brackets in Eq. (9) can be rewritten as

$$\sigma^{-2d+2}d^{2d-2}(2\tilde{k}\tilde{p})^{d-1}\left[1-\left(\frac{\tilde{k}^2+\tilde{p}^2-\tilde{q}^2}{2\tilde{k}\tilde{p}}\right)^2\right]^{(d-3)/2} \times\left(\frac{\tilde{k}^2+\tilde{p}^2-\tilde{q}^2}{2\tilde{k}\tilde{p}}\right)^2 c^2(\tilde{p}d/\sigma). \tag{35}$$

The square bracket in Eq. (35) can be replaced by $e^{-d/2(\tilde{k}^2+\tilde{p}^2-\tilde{q}^2/2\tilde{k}\tilde{p})^2}$. Then, we use

$$x^2e^{-(d/2)x^2}\to\frac{\sqrt{\pi}}{4}\left(\frac{2}{d}\right)^{3/2}\left[\delta\left(x-\sqrt{\frac{2}{d}}\right)+\delta\left(x+\sqrt{\frac{2}{d}}\right)\right], \tag{36}$$

which allows to perform the integration over $\tilde{q}$. Next we account for the asymptotic behavior of $J_n(nx)$ for $n\to\infty$ [20] and obtain from Eq. (11)

$$\begin{aligned}c^2(\tilde{p}d)&=(2\pi)^d\sigma^{2d}d^{-d}J^2_{d/2}[(d/2)2\tilde{p}]/\tilde{p}^d\\&\cong 4(2\pi)^d\sigma^{2d}d^{-d}(\tilde{p}^d\pi d\sqrt{4\tilde{p}^2-1})^{-1}\Theta\left(\tilde{p}-\frac{1}{2}\right)\\&\quad\times\cos^2\left[\frac{d}{2}\sqrt{4\tilde{p}^2-1}-\frac{d}{2}\arctan\sqrt{4\tilde{p}^2-1}-\frac{\pi}{4}\right].\end{aligned} \tag{37}$$

With these simplifications and the fact that $\cos^2[\cdots]$ in Eq. (37) oscillates very fast for d large with average 1/2, we arrive at

$$\tilde{\mathcal{F}}_{\tilde{k}}[\tilde{f}(\tilde{q})]\cong\varphi\frac{2^d}{\tilde{k}^2\pi d}\int_{1/2}^{\infty}d\tilde{p}\frac{\tilde{p}}{\sqrt{4\tilde{p}^2-1}}\tilde{f}(\tilde{p})[\tilde{f}(\tilde{q}_-)+\tilde{f}(\tilde{q}_+)], \tag{38}$$

where

$$\tilde{q}_\pm=\left[\tilde{k}^2+\tilde{p}^2\pm 2\sqrt{\frac{2}{d}}\tilde{k}\tilde{p}\right]^{1/2}. \tag{39}$$

Our first goal will be the evaluation of the critical packing fraction $\varphi_c(d)$. For this we choose $\tilde{k}=\tilde{k}_0\equiv\hat{k}_0d^{1/2}$ such that $\tilde{f}_c(\tilde{k}_0)=1/2$ (see Sec. II C). Equation (26) implies

$$\tilde{\mathcal{F}}_{\tilde{k}_0}[\tilde{f}_c(\tilde{q})]=1,\quad \varphi=\varphi_c(d). \tag{40}$$

$\tilde{f}_c(\tilde{q}_\pm)$ is of order 1 for $\tilde{k}=\tilde{k}_0$ and $\tilde{p}=O(1)$ and decays rapidly to zero for $\tilde{p}\gg 1$. Furthermore, $\tilde{f}(\tilde{p})\cong 1$ for $\tilde{p}=O(1)$. Therefore, the integral in Eq. (38) is of order 1, i.e., order d^0. Then we get from Eq. (38) with $\varphi=\varphi_c(d)$ and $\tilde{k}=\hat{k}\sqrt{d}$,

$$1\cong\tilde{\mathcal{F}}_{\tilde{k}_0}[\tilde{f}_c(\tilde{q})]\cong\pi^{-1}\varphi_c(d)(2^d/d^2)\hat{k}_0^{-2}O(d^0), \tag{41}$$

where $\hat{k}_0$ is of order d^0, as well. Consequently, it must be

$$\varphi_c(d)\cong\text{const}\ d^2 2^{-d}, \tag{42}$$

in agreement with the numerical result for $d\gtrsim 100$ (cf. Fig. 4). Next we choose $\tilde{k}\le\tilde{k}_0$. $\tilde{f}_c(\tilde{q}_\pm)\approx 0$ for $\tilde{q}_\pm>\tilde{k}_0$, which implies

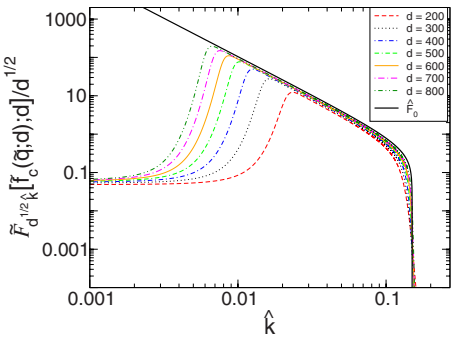

FIG. 7. (Color online) Numerical result for $\tilde{\mathcal{F}}_{\sqrt{d}\hat{k}}[\tilde{f}_c(\tilde{q};d);d]/\sqrt{d}$ as function of $\hat{k}$ for various d. The master function $\hat{F}_0(\hat{k})$ is shown as bold black line.

$$\tilde{p}<\mp\sqrt{2/d}\tilde{k}+\sqrt{(2/d)\tilde{k}^2+(\tilde{k}_0^2-\tilde{k}^2)}\cong\sqrt{(\tilde{k}_0^2-\tilde{k}^2)}$$

for $d\to\infty$ and $\tilde{k}\le\tilde{k}_0$. With $\tilde{f}_c(\tilde{p})[\tilde{f}_c(\tilde{q}_-)+\tilde{f}_c(\tilde{q}_+)]\cong 2$ for $\tilde{p}\lesssim\sqrt{\tilde{k}_0^2-\tilde{k}^2}$, the integration in Eq. (38) can be done. Then we get from Eq. (38) for $\tilde{k}_0-\tilde{k}\gg\hat{k}_0/\sqrt{d}$ after substitution of $\varphi_c(d)$ from Eq. (33)

$$\lim_{d\to\infty}(\tilde{\mathcal{F}}_{\sqrt{d}\hat{k}}[\tilde{f}_c(\tilde{q};d);d]/\sqrt{d})=\hat{F}_0(\hat{k}), \tag{43}$$

with the master function

$$\hat{F}_0(\hat{k})\cong\begin{cases}a\pi^{-1}\hat{k}^{-2}\sqrt{\hat{k}_0^2-\hat{k}^2}, & \hat{k}\le\hat{k}_0\\ 0, & \hat{k}>\hat{k}_0.\end{cases} \tag{44}$$

Figure 7 presents the numerically exact result for $\tilde{\mathcal{F}}_{\sqrt{d}\hat{k}}[\tilde{f}_c(\tilde{q};d);d]/\sqrt{d}$ as function of $\hat{k}=k\sigma/d^{3/2}$.

This figure demonstrates the convergence of $\tilde{\mathcal{F}}_{\sqrt{d}\hat{k}}/\sqrt{d}$ at the glass transition singularity to the master function $\hat{F}_0(\hat{k})$. For $\hat{k}<\hat{k}_0$, i.e., $\tilde{k}<\tilde{k}_0$, the critical nonergodicity parameters $\tilde{f}_c(\tilde{k};d)$ are close to one for $d\to\infty$. Making use of Eqs. (26) and (43), the $\tilde{k}$ and d dependences of $\tilde{f}_c(\tilde{k};d)$ can be expressed as follows:

$$\tilde{f}_c(\tilde{k};d)\cong\frac{\sqrt{d}\hat{F}_0(\tilde{k}/\sqrt{d})}{1+\sqrt{d}\hat{F}_0(\tilde{k}/\sqrt{d})}, \tag{45}$$

i.e., on the scale $\hat{k}=k\sigma/d^{3/2}$ it is

$$\lim_{d\to\infty}f_c[(d^{3/2}/\sigma)\hat{k};d]\equiv\hat{f}_c(\hat{k})=\Theta(\hat{k}_0-\hat{k}). \tag{46}$$

The convergence of the critical nonergodicity parameters to a step function is demonstrated in Fig. 8.

IV. SUMMARY AND CONCLUSIONS

The liquid-glass transition for hard spheres in high dimensions d has been reinvestigated in the framework of MCT. Our aim has not been exploring the validity of the MCT approximations for $d\to\infty$ (we come back to this point below) but to take MCT as a microscopic theory in any dimen-

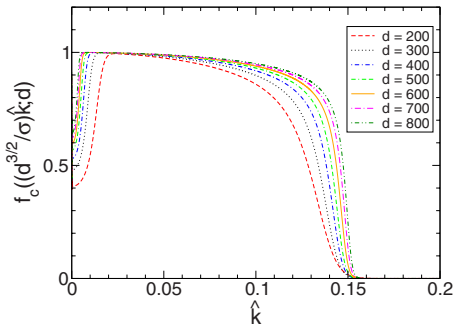

FIG. 8. (Color online) Numerical critical nonergodicity parameters on the scale $\hat{k}=k\sigma/d^{3/2}$ for various dimensions d.

sion and to check the generic MCT-bifurcation scenario (A_2 singularity) and to calculate the critical packing fraction, the corresponding nonergodicity parameters, and the exponent parameter. The direct correlation function for hard (hyper-) spheres for finite d is not known exactly. However, if $\varphi = O[\varphi_c(d)] \sim d^2 2^{-d}$, being exponentially smaller than $\varphi_*(d)$ at which the Kirkwood-like instability occurs, the corrections to the leading-order result [Eq. (11)] can be neglected for $d \to \infty$. This offers the possibility to calculate various quantities such as $\varphi_c(d)$, $f_c(k;d)$, $f_c^{(s)}(k;d)$, and $\lambda(d)$ from MCT for a liquid of hard spheres in high dimensions.

A. Summary

Let us first summarize our results. The numerical solution of the MCT equations for the collective and self-nonergodicity parameters up to $d=800$ reveals non-Gaussian dependence of the critical nonergodicity parameters $f_c(k)$ and $f_c^{(s)}(k)$ on the wave number k (cf. Fig. 5). Three different k scales were found on which $f_c(k)$ behaves differently. For $k\sigma=O(\sqrt{d})$, $f_c(k)$ increases from $f_c(0)<1$ to a maximum value close to 1. $f_c(k)$ stays close to 1 for $k\sigma=O(d)$ and finally drops to zero for $k\sigma \cong \hat{k}_0 d^{3/2}$. The decrease to zero happens on the scale $\hat{k}=k\sigma/d^{3/2}$ in an interval around $\hat{k}_0$ with width of order $1/d$. $f_c^{(s)}(k)$ and $f_c(k)$ are identical for $k\sigma = O(d)$ but differ for $k\sigma=O(d^{1/2})$. The exponent parameter $\lambda(d)$ (cf. Fig. 6) varies with d even for $d>100$ and strongly exceeds the value $\lambda(3) \cong 0.735$ [25] for $d \gg 1$. Note that $\lambda(d)$ cannot be larger than 1. The critical amplitudes $h(k;d)$ [3] exhibit the expected k dependence. They are in antiphase with $f_c(k;d)$, i.e., they have a maximum (minimum) where $f_c(k;d)$ has a minimum (maximum). Particularly, on the scale $k\sigma=O(d)$, the critical amplitudes are rather small since $f_c(k;d) \approx 1$. The numerical results (up to $d=800$) also show that the largest eigenvalue $E_0(\varphi)$ of the stability matrix [3] is not degenerate and it approaches the bifurcation point at $\varphi_c(d)$ as $[1-E_0(\varphi)] \sim \sqrt{[\varphi-\varphi_c(d)]/\varphi_c(d)}$, for $\varphi \to \varphi_c(d)$ from above. Hence, the glass transition singularity is an A_2 singularity, consistent with an exponent parameter $\lambda(d)$ smaller than 1, as demonstrated by Fig. 6. What happens for $d=\infty$ is not clear. The distances between the largest eigenvalues of the stability matrix obtained numerically slightly decrease with increasing d. Whether or not the largest eigenvalue becomes degenerate for $d=\infty$ is an open question, similar to the question whether $\lambda(d)$ in Fig. 6 converges to one for $d \to \infty$ or not. Therefore, our numerical results do not allow to exclude a higher-order singularity at $d=\infty$.

Inspired by these numerical results, we have been able to prove analytically that the Vineyard approximation [15] becomes exact for $d \to \infty$ on a scale $k\sigma=O(d)$ and that the critical packing fraction $\varphi_c(d)$ decays exponentially as 2^{-d}, with a prefactor which is quadratic in d. This is consistent with the numerical result for $d \gtrsim 100$. Furthermore, the analytical approach has also shown that the k and d dependences of the critical nonergodicity parameters and of the MCT functional $\tilde{\mathcal{F}}_{\tilde{k}}[\tilde{f}_c(\tilde{q};d);d]$ at $\varphi_c(d)$ can be obtained from a master function $\hat{F}_0(\hat{k})$ [cf. Eqs. (43) and (45)]. This relationship yields

$$\lim_{d\to\infty} f_c(\hat{k}\sigma^{-1}d^{3/2};d) = \Theta(\hat{k}_0 - \hat{k}), \quad d \to \infty, \tag{47}$$

where $\hat{k}_0 \cong 0.15$.

B. Validity of MCT

Although it has not been our purpose to prove or disprove the validity of MCT for $d \to \infty$, it might be useful to comment on this question. First of all, the vertices (7) and (9) seem to be exact for $d \to \infty$, since the leading order of $c(k;d,\varphi)$ is known analytically and the neglect of the triplet direct correlation function $c^{(3)}(\vec{p},\vec{q})$, which also enters into the vertices [3], is justified for $\varphi \sim d^2 2^{-d}$ and $d \to \infty$ (see the Appendix). Accordingly, the convolution approximation for the static three-point correlator $\langle \rho(\vec{k})^* \rho(\vec{p}) \rho(\vec{q}) \rangle$ (usually done in MCT) becomes exact for $d \to \infty$ and packing fractions such that $2^d \varphi(d)$ does not increase exponentially or faster with d. The factorization of the static four-point density correlator $S^{(4)}(\vec{q}_1,\vec{q}_2,\vec{q}_3,\vec{q}_4) = \frac{1}{N}\langle \rho^*(\vec{q}_1)\rho^*(\vec{q}_2)\rho(\vec{q}_3)\rho(\vec{q}_4)\rangle$, which is needed for the projector onto pairs of density modes, is another approximation. Similar to $S^{(3)}(\vec{p},\vec{q}) = \frac{1}{N}\langle \rho(\vec{p}+\vec{q})^* \rho(\vec{p})\rho(\vec{q})\rangle$ (see the Appendix), one can define a quadruplet direct correlation function $c^{(4)}(\vec{q}_1,\vec{q}_2,\vec{q}_3)$ via a corresponding Ornstein-Zernike equation. However, this equation is already rather involved [26] such that we have not attempted to prove that the factorization is valid for $\varphi=\varphi_c(d)$ and $d \to \infty$. So it remains an open question whether this factorization becomes exact again. If so, the "only" two remaining crucial approximations of MCT are the projection of the fluctuating force onto pair modes and the subsequent factorization of the pair density correlator with reduced dynamics into a product of density correlators $\phi(k,t)$ with full dynamics. Whether these two steps become exact for $d \to \infty$ is an interesting but also a highly nontrivial question. Activated processes smear out the glass transition singularity. Since it seems that the local barriers between adjacent metastable configurations increase with increasing d (see also Ref. [18]), these hopping processes may become suppressed for $d \to \infty$. Even if this is true, it is not obvious that the remaining two approximations of MCT become exact for $d \to \infty$.

One might conclude that MCT for $d \to \infty$ necessarily fails because of $S[k;d,\varphi_c(d)] \cong 1$ for $k\sigma=O(d)$, excluding the cage effect [3] as driving mechanism, and one may argue that

the dynamics will be described better by a Boltzmann-Enskog equation. Indeed, a modified Enskog equation was derived from the binary-collision expansion [27]. But its validity for packing fractions of order 2^{-d} has not been proven. Here, two comments are in order. *First*, a cage does not necessarily require a maximum number of adjacent spheres. For instance, a (simple) hypercubic lattice built up of periodically arranged hyperspheres has $2d$ nearest neighbors and a volume fraction $\varphi_{\text{hypercube}}(d) \sim d^{-d/2}$, which is much smaller than $\varphi_c(d) \sim 2^{-d}$. Therefore, the number of contacts between neighbors for $\varphi = \varphi_c(d)$ could be large enough in order to have a cage. Furthermore there is evidence that the packing fraction $\varphi_{\text{MRJ}}(d)$ for maximally random jammed states in d dimensions is given by $(c_1 + c_2 d)2^{-d}$ [28] or even with an additional term with a quadratic prefactor $c_3 d^2$ [29]. These densities are not larger than $\varphi_c(d)$. The corresponding pair-correlation function $g_2(r;d)$ flattens under an increase of d from 3 to 6 [28], i.e., comes closer to the ideal-gas value $g_{ig}(r;d) = 1$ for $r > \sigma$. *Second*, concerning MCT $S[k;d,\varphi_c(d)] \cong 1$ does not imply that the direct correlation function $c[k;d,\varphi_c(d)]$ and the vertices are zero. It is the quadratic dependence of the vertices on $c(k;d,\varphi)$ in combination with its explicit n dependence and the use of the scaled variables $\tilde{k} = k\sigma/d$ which make the coupling of the modes finite despite the small packing fraction $\varphi_c(d) \sim d^2 2^{-d}$. This is completely similar to the MCT approach to colloidal gelation for a liquid of hard spheres with attractive Yukawa potential [30,31]. For packing fraction $\varphi \to 0$ and potential strength $K \to \infty$ with $K\varphi^2 = \Gamma = \text{const}$, these authors prove that $S(k) \to 1$ for all k. However, the vertices remain finite. At a critical value Γ_c, a liquid-gel transition occurs. $f_c(k)$ is similar to $f_c^{(s)}(k)$, quite analogous to our outcome. The equilibrium structure at Γ_c is highly ramified where the "caging" of a sphere is generated by a smaller number of neighbors.

C. Conclusions

In Sec. IV A, we have presented our various results from MCT in high dimensions. Now we want to discuss the most essential findings in the light of earlier results and will draw some conclusions.

Our critical nonergodicity parameters have a non-Gaussian k dependence, in variance with the assumption in Ref. [16]. This discrepancy is the origin of the different pre-exponential factor of the critical packing fraction which we have found to be quadratic in d and not linear [16]. Due to this quadratic d dependence, our MCT result for $\varphi_c(d)$ is larger than the Kauzmann packing fraction $\varphi_K(d)$ [Eq. (2)]. This cannot be true since the packing fraction for the Kauzmann transition (static glass transition) should be above the packing fraction for the MCT transition (dynamical glass transition). $\varphi_K(d)$ has been calculated within a small cage expansion [18], which is a kind of Gaussian approximation. This could be the reason why $\varphi_K(d)$ [Eq. (2)] is below $\varphi_c(d)$ [Eq. (33)].

As argued in Sec. IV B, it is not necessarily true that a structureless static correlator rules out caging. But, even if the cage effect would be absent, the essential question would be whether the quality of both MCT approximations *necessarily* requires the existence of caging or not. Since an analytical investigation of the validity of these approximations seems to be extremely difficult, a way to get an insight is an approach by a computer simulation. Provided such simulational results would deviate more and more from our results with increasing dimensions, this would hint at a failure of MCT for $d \to \infty$. Such a failure would imply that MCT, which has been interpreted as a mean-field theory [11], does not become exact in the limit of high dimensions, in contrast to equilibrium phase transitions. We hope that these concluding remarks may stimulate and encourage further investigations, contributing to a better understanding of MCT.

ACKNOWLEDGMENTS

We would like to thank K. Binder, T. Franosch, M. Fuchs, and W. Schirmacher for stimulating discussions. The numerous helpful comments on our paper by G. Biroli, W. Götze, and F. Zamponi are gratefully acknowledged as well.

APPENDIX

We want to prove the following statement: for all packing fractions $\varphi(d)$ such that $2^d\varphi(d)$ does not increase exponentially or faster with d for $d \to \infty$, the static three-point correlation function $S^{(3)}(\vec{k},\vec{k}')$ reduces in the limit of high dimensions to $S(k)S(k')S(|\vec{k}+\vec{k}'|)$, i.e., the convolution approximation becomes exact. For this proof, we use the Ornstein-Zernike equation for three-particle correlation functions [32]

$$S^{(3)}(\vec{k},\vec{k}') = S(k)S(k')S(|\vec{k}+\vec{k}'|)[1 + n^2 c^{(3)}(\vec{k},\vec{k}')]. \quad \text{(A1)}$$

So, we have to show that $n^2 c^{(3)}(\vec{k},\vec{k}') \to 0$ for all $\vec{k}$, $\vec{k}'$ for $d \to \infty$ and φ constrained as above. The explicit dependence of $c^{(3)}(\vec{k},\vec{k}')$ on $\vec{k}$, $\vec{k}'$ does not have to be considered, as we can use for all $\vec{k}$, $\vec{k}'$,

$$n^2|c^{(3)}(\vec{k},\vec{k}')| = n^2\left|\int d^d r \int d^d r' e^{-i\vec{k}\vec{r}} e^{-i\vec{k}\vec{r}'} c^{(3)}(\vec{r},\vec{r}')\right|$$

$$\leq n^2 \int d^d r \int d^d r' |c^{(3)}(\vec{r},\vec{r}')|. \quad \text{(A2)}$$

Now we can expand $c^{(3)}(\vec{r},\vec{r}')$ into diagrams, where the lines are Mayer functions and the vertices are single-particle densities. This expansion only consists of loop diagrams. We want to show now that the contribution of each of these diagrams to $n^2 \int d^d r \int d^d r' |c^{(3)}(\vec{r},\vec{r}')|$ vanishes in the limit $d \to \infty$. To do so, we apply the theorem of Wyler *et al.* [2]. This theorem states that a loop diagram leads to an exponentially smaller contribution to an integral like the one appearing in the last line of Eq. (A2) than a tree diagram of the same order. The simplest diagram in the expansion of $c^{(3)}(\vec{r},\vec{r}')$ reads

$$|c_0^{(3)}(\vec{r},\vec{r}')| = \Theta(\sigma - r)\Theta(\sigma - r')\Theta(\sigma - |\vec{r} - \vec{r}'|), \quad \text{(A3)}$$

which can be inserted into Eq. (A2)

$$|c_0^{(3)}(\vec{k},\vec{k}')| \le \int d^d r \int d^d r' \Theta(\sigma - r)\Theta(\sigma - r')\Theta(\sigma - |\vec{r} - \vec{r}'|). \tag{A4}$$

The integral occurring in Eq. (A4) leads to an exponentially smaller contribution than the corresponding tree diagram of the same order [2]

$$\int d^d r \int d^d r' \Theta(\sigma - r)\Theta(\sigma - r')\Theta(\sigma - |\vec{r} - \vec{r}'|) \le \alpha^d \int d^d r \int d^d r' \Theta(\sigma - r)\Theta(\sigma - r') = \alpha^d [V_d(\sigma)]^2, \tag{A5}$$

where $V_d(\sigma)$ is the volume of a d-dimensional sphere with radius σ and

$$\alpha < 1. \tag{A6}$$

From Eqs. (A4) and (A5), we obtain

$$n^2 |c_0^{(3)}(\vec{k},\vec{k}')| \le \alpha^d [n V_d(\sigma)]^2. \tag{A7}$$

Together with

$$\varphi = n V_d\left(\frac{\sigma}{2}\right) = 2^{-d} n V_d(\sigma), \tag{A8}$$

this leads to

$$n^2 |c_0^{(3)}(\vec{k},\vec{k}')| \le \alpha^d (2^d \varphi)^2, \tag{A9}$$

i.e., for all packing fractions, where $2^d\varphi$ does not increase exponentially or faster with d, we obtain from Eqs. (A6) and (A9)

$$n^2 |c_0^{(3)}(\vec{k},\vec{k}')| \underset{d\to\infty}{\to} 0 \quad \text{for all } \vec{k},\ \vec{k}'. \tag{A10}$$

The contributions of all other diagrams are also exponentially smaller than the corresponding tree diagrams [2], which leads to

$$n^2 |c_i^{(3)}(\vec{k},\vec{k}')| \le \alpha_i^d n^2 [V_d(\sigma)]^2 n^j [V_d(\sigma)]^j, \tag{A11}$$

where j is the number of vertices over which it has to be integrated in the corresponding diagram and α_i is always smaller than one. From this we obtain

$$n^2 |c_i^{(3)}(\vec{k},\vec{k}')| \le \alpha_i^d (2^d \varphi)^{j+2} \tag{A12}$$

or

$$n^2 |c_i^{(3)}(\vec{k},\vec{k}')| \underset{d\to\infty}{\to} 0 \quad \text{for all } \vec{k},\vec{k}' \text{ and all } i, \tag{A13}$$

provided $2^d\varphi(d)$ does not increase exponentially or faster with d.

[1] H. L. Frisch, N. Rivier, and D. Wyler, Phys. Rev. Lett. **54**, 2061 (1985).
[2] D. Wyler, N. Rivier, and H. L. Frisch, Phys. Rev. A **36**, 2422 (1987).
[3] W. Götze, *Complex Dynamics of Glass-Forming Liquids: A Mode-Coupling Theory* (Oxford University Press, Oxford, 2009).
[4] W. van Megen and S. M. Underwood, Phys. Rev. Lett. **70**, 2766 (1993); W. van Megen, Transp. Theory Stat. Phys. **24**, 1017 (1995).
[5] M. Sperl, Phys. Rev. E **71**, 060401(R) (2005).
[6] M. Bayer, J. M. Brader, F. Ebert, M. Fuchs, E. Lange, G. Maret, R. Schilling, M. Sperl, and J. P. Wittmer, Phys. Rev. E **76**, 011508 (2007).
[7] D. Hajnal, J. M. Brader, and R. Schilling, Phys. Rev. E **80**, 021503 (2009).
[8] R. Brüning, D. A. St.-Onge, S. Patterson, and W. Kob, J. Phys.: Condens. Matter **21**, 035117 (2009).
[9] J. D. Eaves and D. R. Reichman, Proc. Natl. Acad. Sci. U.S.A. **106**, 15171 (2009).
[10] P. Charbonneau, A. Ikeda, J. van Meel, and K. Miyazaki, e-print arXiv:0909.1952.
[11] G. Biroli and J.-P. Bouchaud, Europhys. Lett. **67**, 21 (2004).
[12] G. Biroli and J.-P. Bouchaud, J. Phys.: Condens. Matter **19**, 205101 (2007).
[13] S. Franz, G. Parisi, F. Ricci-Tersenghi, and T. Rizzo, e-print arXiv:1001.1746.
[14] A. Andreanov, G. Biroli, and J.-P. Bouchaud, Europhys. Lett. **88**, 16001 (2009).
[15] J. Boon and S. Yip, *Molecular Hydrodynamics* (McGraw-Hill, New York, 1980).
[16] T. R. Kirkpatrick and P. G. Wolynes, Phys. Rev. A **35**, 3072 (1987).
[17] M. Mézard and G. Parisi, J. Phys A **29**, 6515 (1996); e-print arXiv:0910.2838.
[18] G. Parisi and F. Zamponi, J. Stat. Mech.: Theory Exp. (2006), P03017.
[19] H. L. Frisch and J. K. Percus, Phys. Rev. E **60**, 2942 (1999).
[20] M. Abramowitz and I. A. Stegun, *Handbook of Mathematical Functions* (Dover Publications, New York, 1970).
[21] The result (22) for $\varphi_*(d)$ has already been obtained earlier [19,22,23], however, with different numerical prefactors. The prefactor of Frisch and Percus [19,22] $c_0 \cong 0.871$ agrees to our prefactor if one inserts the correct value of the derivative of the Airy function: $A_i'(-2^{1/3}a_0) \cong 0.701\,211$. The prefactor obtained by Bagchi and Rice [23] is $c_0 \cong 0.239$.
[22] H. L. Frisch and J. K. Percus, Phys. Rev. A **35**, 4696 (1987).
[23] B. Bagchi and S. A. Rice, J. Chem. Phys. **88**, 1177 (1988).
[24] A. Winkler, A. Latz, R. Schilling, and C. Theis, Phys. Rev. E **62**, 8004 (2000).
[25] T. Franosch, M. Fuchs, W. Götze, M. R. Mayr, and A. P. Singh, Phys. Rev. E **55**, 7153 (1997).
[26] L. L. Lee, J. Chem. Phys. **60**, 1197 (1974).
[27] Y. Elskens and H. L. Frisch, Phys. Rev. A **37**, 4351 (1988).

[28] M. Skoge, A. Donev, F. H. Stillinger, and S. Torquato, Phys. Rev. E **74**, 041127 (2006).
[29] A. P. Philipse, Colloids Surf., A **213**, 167 (2003).
[30] J. Bergenholtz and M. Fuchs, Phys. Rev. E **59**, 5706 (1999); J. Phys.: Condens. Matter **11**, 10171 (1999).
[31] J. Bergenholtz, M. Fuchs, and Th. Voigtmann, J. Phys.: Condens. Matter **12**, 6575 (2000).
[32] J.-L. Barrat, J.-P. Hansen, and G. Pastore, Mol. Phys. **63**, 747 (1988).